

Stopping power of nonideal, partially ionized plasmas

D. O. Gericke*

Theoretical Division, Los Alamos National Laboratory, Los Alamos, New Mexico 87545

M. Schlanges

Institut für Physik, Ernst-Moritz-Arndt-Universität Greifswald, Domstraße 10a, 17487 Greifswald, Germany

Th. Bornath

Fachbereich Physik, Universität Rostock, Universitätsplatz 3, 18051 Rostock, Germany

(Received 10 July 2001; published 15 February 2002)

The stopping power of strongly coupled, partially ionized plasmas is investigated for charged beam particles with arbitrary velocities. Our approach is based on kinetic equations of the Boltzmann type that are suitably generalized to describe three-particle collisions. In this way, we consider elastic collisions between the beam and free plasma particles as well as the ionization and excitation of composite plasma particles by beam particle impact. Explicit expressions for both contributions are given in terms of the momentum transfer cross section that has been generalized for three-particle collisions. For fast beam particles, we obtain a generalized Bethe formula that includes correction terms due to the nonideality of the target plasma. Results are shown for hydrogen, carbon, and argon plasmas. Considerable modifications compared to the ideal behavior arise for strongly coupled plasmas. In particular, we are able to describe the Mott transition in the stopping power of dense, partially ionized plasmas.

DOI: 10.1103/PhysRevE.65.036406

PACS number(s): 52.40.Mj, 52.25.Fi, 52.27.Gr, 52.20.Hv

I. INTRODUCTION

Beam-matter interaction experiments are one of the key tools to investigate the properties of dense plasmas. One field of interest is the creation and heating of plasmas. Here, special focus is directed to inertial confinement fusion related topics, e.g., to the properties in heavy ion fusion converters [1,2], to α -particle heating in the fusion core [3,4], and to fast ignition by proton beams [5]. Furthermore, heavy ion beams can be used to produce cold, dense plasmas for equation of state investigations [6,7]. To guide and to interpret these experiments, a precise knowledge of the energy loss of charged particles traveling through strongly coupled plasmas is needed. The diagnostics of dense plasmas [8,9] is another important application of particle beams where an exact description of the stopping power is required.

Except high-temperature hydrogen plasmas, most of the target plasmas under consideration in these experiments and applications are partially ionized. Therefore, descriptions of both the contribution due to the free plasma particles and the one due to the bound electrons or composite particles have to be considered.

In recent years much theoretical work has been done to model the interaction between beam ions and free plasma particles in nonideal plasmas. For instance, local field corrections [10], density functional theory [11,12], the force autocorrelation function [13], the nonlinear system of Vlasov-Poisson equations [14], kinetic equations beyond the Born approximation [15–17], and computer simulations [18,19] have been applied. In these investigations, special attention was paid to strong beam ion-plasma electron correlations.

Furthermore, the energy loss of correlated beam ions as well as cluster ion beams was investigated (see, e.g., Refs. [20,21]).

Although the first calculations for the stopping power were done for gas targets [22–24], much less theoretical work has been done for the bound state contribution in plasma targets. Most of the approaches result in a modified Bethe formula that is generalized for multiply charged plasma ions (see, e.g., [25–27]). For weakly coupled plasmas and fast ion beams, this formula is in good agreement with experimental data [8,28], however, deviations arise for higher particle densities [29]. A modified Bethe formula has been also derived for the energy loss of electron beams in dense plasmas [30].

In this paper, we pay special attention to the bound electron contribution. For this purpose, we utilize kinetic equations of the Boltzmann type including three-particle collisions [31,32]. This approach is particularly advantageous because it allows the inclusion of all relevant two- and three-particle scattering processes in a systematic way. The considered kinetic equations also include strong coupling effects as the lowering of the ionization energy and medium effects on the cross sections [33,34]. Furthermore, no approximations concerning the beam particle velocity are necessary.

To give a general insight into this approach, a brief discussion of the kinetic equations is given in Sec. II. On this basis, we derive explicit expressions for the ionization, excitation, and deexcitation contributions to the stopping power in Sec. III. Furthermore, a description of the calculation of the ionization and excitation cross sections, which are the main input quantities, is given in this section. The free electron contribution is addressed in the next section. For this contribution, we use a scheme that considers close collisions as well as dynamic screening effects [16,17]. Results for

*Electronic address: gericke@lanl.gov

strongly coupled hydrogen plasmas are given in Sec. V A. The effect of the plasma composition on the stopping power of carbon plasmas is investigated in Sec. V B. Furthermore, a comparison with experimental data for an argon plasma is shown.

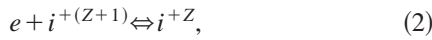
II. KINETIC EQUATIONS FOR PARTIALLY IONIZED PLASMAS

Before we turn to the calculation of the stopping power, let us briefly discuss our approach to the properties of partially ionized plasmas. We employ the so-called chemical picture, i.e., the basic elements of our analysis are free electrons, free ions, and composite particles. The latter can be atoms or ions. Applying the kinetic description, the properties of the system can be expressed in terms of the distribution functions for free carriers $f_a(\mathbf{p}, t)$ and composite particles (two-particle bound states) $F_j(\mathbf{P}, t)$, where the index “ j ” denotes a complete set of internal quantum numbers. These distributions are normalized as follows:

$$n_a = \int \frac{d\mathbf{p}}{(2\pi\hbar)^3} f_a(\mathbf{p}, t) \quad \text{and} \quad n_j = \int \frac{d\mathbf{P}}{(2\pi\hbar)^3} F_j(\mathbf{P}, t). \quad (1)$$

Here, n_a is the free carrier number density of the species “ a ,” and n_j is the number density of the composite particles in the state $|j\rangle$. The total density of bound states is given by $n^b = \sum_j n_j$. Then it holds for the total electron density: $n_e^{\text{tot}} = n_e + n^b$.

To describe the balance between the different species, one has to consider the possibility of reactions between the particles, e.g., ionization and recombination



and inelastic processes changing only the internal state (excitation and deexcitation). It is well known that energy and momentum conservation in such inelastic scattering processes require at least three particles. Therefore, one has to go beyond the usually used binary collision approximation in order to describe partially ionized plasmas including such inelastic processes.

The time evolution of the free and bound particle distribution has to be determined by a set of appropriate kinetic

TABLE I. Definitions of multichannel scattering theory for the different types of three-particle collisions: channel index k , asymptotic states $|k\alpha\rangle$, differentials, three-particle energies, and the set of distribution functions in the considered channel.

k	$ k\alpha\rangle$	$d(k\alpha)$	E_{abc}^k	$f_k(k\alpha)$
0	$ \mathbf{p}_a\rangle \mathbf{p}_b\rangle \mathbf{p}_c\rangle$	$d\mathbf{p}_a d\mathbf{p}_b d\mathbf{p}_c$	$E_a + E_b + E_c$	$f_a(\mathbf{p}_a) f_b(\mathbf{p}_b) f_c(\mathbf{p}_c)$
1	$ \mathbf{p}_a\rangle \mathbf{P}_{bcj}\rangle$	$d\mathbf{p}_a d\mathbf{P}_{bc}$	$E_a + E_{bc}$	$f_a(\mathbf{p}_a) F_j(\mathbf{P}_{bc})$
2	$ \mathbf{p}_b\rangle \mathbf{P}_{acj}\rangle$	$d\mathbf{p}_b d\mathbf{P}_{ac}$	$E_b + E_{ac}$	$f_b(\mathbf{p}_b) F_j(\mathbf{P}_{ac})$
3	$ \mathbf{p}_c\rangle \mathbf{P}_{abj}\rangle$	$d\mathbf{p}_c d\mathbf{P}_{ab}$	$E_c + E_{ab}$	$f_c(\mathbf{p}_c) F_j(\mathbf{P}_{ab})$

equations that account for all relevant two- and three-particle processes. Furthermore, the influence of the surrounding medium on the scattering processes has to be included in the case of strongly coupled plasmas. Kinetic equations considering inelastic scattering processes as well as many-particle effects were derived in the frame of density operator formalism [35–38] and using the technique of nonequilibrium Green’s functions [31,39–41]. The latter approach is based on a cluster expansion of the two-particle Green’s function including self-energies and phase space occupation effects.

The result is a generalized Boltzmann equation containing additional three-particle collision integrals. Due to the screening of the Coulomb potential, the effective interaction in dense plasmas is short ranged. Therefore, kinetic equations of the Boltzmann type can be applied also for partially ionized plasmas [40,41]. In the case of homogeneous and isotropic plasmas, the resulting kinetic equation for the free carriers reads

$$\frac{\partial}{\partial t} f_a(\mathbf{p}, t) = \sum_b I_{ab}(\mathbf{p}, t) + \sum_{bc} I_{abc}(\mathbf{p}, t). \quad (3)$$

For inhomogeneous or anisotropic plasmas, the left-hand side (lhs) has to be replaced by the well-known drift term.

The right-hand side (rhs) of Eq. (3) contains the different collision terms. The first term describes the scattering of two free carriers. Depending on the applied approximation scheme, it is given, e.g., by the collision integral of the Lenard-Balescu [42,43] or Boltzmann kinetic equations [44]. The second sum on the rhs includes the different three-particle scattering processes. Considering a nondegenerate plasma, this three-particle collision integral is given by [31,36]

$$\begin{aligned} I_{abc}(\mathbf{p}_a, t) &= \frac{1}{V\hbar} \sum_{b,c} \sum_k \int \frac{d\mathbf{p}_b}{(2\pi\hbar)^3} \frac{d\mathbf{p}_c}{(2\pi\hbar)^3} d(k\bar{\alpha}) |\langle \mathbf{p}_a | \langle \mathbf{p}_b | \langle \mathbf{p}_c | T_{abc}^{0k} | k\bar{\alpha} \rangle|^2 \\ &\quad \times 2\pi \delta(E_{abc}^0 - \bar{E}_{abc}^k) \{ f_k(k\bar{\alpha}, t) - f_a(\mathbf{p}_a, t) f_b(\mathbf{p}_b, t) f_c(\mathbf{p}_c, t) \} \\ &\quad + \frac{1}{V\hbar} \sum_{b,c} \sum_k \int \frac{d\mathbf{P}_{bc}}{(2\pi\hbar)^3} d(k\bar{\alpha}) |\mathbf{p}_a | \langle \mathbf{P}_{bcj} | T_{abc}^{1k} | k\bar{\alpha} \rangle|^2 \\ &\quad \times 2\pi \delta(E_{abc}^1 - \bar{E}_{abc}^k) \{ f_k(k\bar{\alpha}, t) - f_a(\mathbf{p}_a, t) F_j(\mathbf{P}_{bc}, t) \}. \end{aligned} \quad (4)$$

In this expression, we used the notations of multichannel scattering theory that are explained in Table I (see also Refs. [45,46]). The index “ k ” denotes the scattering channel that corresponds to the channel state $|k\bar{\alpha}\rangle$. In this way, the summation over k accounts for all kinds of scattering processes: the first main term describes all processes with three free particles in the incoming channel (e.g., three-particle recombination) whereas the second one considers all processes with one bound and one free particle in the incoming channel (e.g., impact ionization).

E_{abc}^k are the quasiparticle energies for three particles in the channel k that are explained in Table I. For the one- and two-particle energies mentioned in this table, we have

$$E_a = \frac{p_a^2}{2m_a} + \Delta_a \quad (5)$$

and

$$E_{ab} = \frac{P_{ab}^2}{2M_{ab}} + E_j + \Delta_{ab}^j. \quad (6)$$

In the latter definition, E_j denotes the binding energy of an isolated state $|j\rangle$. The influence of the surrounding medium is reflected by the energy shifts Δ_a and Δ_{ab}^j . In order to simplify the calculation, momentum independent shifts in rigid shift approximation [47] are used frequently. In this approximation, the energy shifts can be identified with the correlation part of the chemical potential μ , i.e., $\mu = \mu^{\text{ideal}} + \Delta$. Assuming statically screened Coulomb interactions, the shifts are given in lowest order in the density by

$$\Delta_a(t) = -\frac{Z_a e^2 \kappa(t)}{2}. \quad (7)$$

Here, $\kappa^2 = 4\pi e^2 \sum_c Z_c^2 n_c / k_B T$ is the (local) inverse Debye screening length. However, one has to go beyond approximation (7) for strongly coupled systems. In this case, more sophisticated approximations have to be applied [48].

The transition probabilities from a given channel k to an outgoing channel \bar{k} are described by the retarded three-particle T matrices $T_{abc}^{k\bar{k}}$, where the energy arguments are fixed on the energy shell of the considered scattering process. These T matrices obey the following Lippmann-Schwinger equation (operator notation) [39,45]:

$$T_{abc}^{k\bar{k}}(\omega) = V_{abc}^k + V_{abc}^k G_{abc}^R(\omega) V_{abc}^{\bar{k}}, \quad (8)$$

where $G_{abc}^R = (\omega - H_{abc}^0 - V_{abc}^0 + i\epsilon)^{-1}$ is the retarded three-particle Green's function, and H_{abc}^0 is the effective free three-particle Hamiltonian including self-energy effects via the energy shifts. The channel potentials V_{abc}^k are given in terms of the effective (screened) two-particle interaction potential V_{ab} ,

$$V_{abc}^0 = V_{ab} + V_{ac} + V_{bc}, \quad (9)$$

$$V_{abc}^1 = V_{ab} + V_{ac}, \quad (10)$$

etc.

However, Eq. (3) for the free carrier distribution is not closed. Furthermore, an equation for the distribution of the composite particles $F_j(\mathbf{P}_{ab}, t)$ is needed to describe the time evolution of a partially ionized plasma. For homogeneous and isotropic systems, this kinetic equation reads [39,41]

$$\frac{\partial}{\partial t} F_j(\mathbf{P}_{ab}, t) = \sum_c I_{abc}^j(\mathbf{P}_{ab}, t). \quad (11)$$

\mathbf{P}_{ab} denotes here the total momentum of the composite particle “ (ab) .” For inhomogeneous and anisotropic systems, the lhs of Eq. (11) has to be replaced by the drift term for a two-particle complex. The rhs is a collision integral that describes the interaction of a bound particle complex with a free carrier. For nondegenerate systems, we have for this collision integral

$$\begin{aligned} I_{abc}^j(\mathbf{P}_{ab}, t) = & \frac{1}{V\hbar} \sum_{c,k} \int \frac{d\mathbf{p}_c d(k\bar{\alpha})}{(2\pi\hbar)^3} 2\pi \delta(E_{abc}^3 - \bar{E}_{abc}^k) \\ & \times |\langle \mathbf{p}_c \mathbf{P}_{abj} | T_{abc}^{3k} | k\bar{\alpha} \rangle|^2 \\ & \times \{f_k(k\bar{\alpha}, t) - F_j(\mathbf{P}_{ab}, t) f_c(\mathbf{p}_c, t)\}. \end{aligned} \quad (12)$$

The notation of multichannel scattering theory is used here again (see Table I). The index “ c ” denotes a species of free plasma particles scattering with the bound complex.

The system of equations (3) and (11) with the collision integrals (4) and (12) allows the description of partially ionized plasmas considering the following scattering processes: elastic two- and three-particle collisions, elastic carrier-bound state collisions, rearrangement processes, impact ionization by free carriers, three-particle recombination, and excitation and deexcitation due to particle impact.

Furthermore, this system considers dense plasma effects included in the quasiparticle energies and in the three-particle T matrices $T_{abc}^{k\bar{k}}$. Therefore, the presented kinetic equations are an appropriate basis to derive expressions for the stopping power of partially ionized plasmas including many-particle effects.

III. BOUND STATE CONTRIBUTION TO THE STOPPING POWER

In this paper, we investigate the energy loss of beam particles with a fixed beam charge number Z_b neglecting their inner structure. That means, that we do not consider the evolution of the beam particle charge. This approximation is appropriate for short times and in the case of beams consisting of electrons, protons, and fast nuclei of light elements, where the beam charge number remains almost constant. However, the stopping power of heavy ions can also be described in many cases considering the (velocity dependent) equilibrium charge state of the considered beam particle species [49].

For the beam particle distribution f_b , we use a delta-function-like distribution in momentum space,

$$f_b(\mathbf{p}) = (2\pi\hbar)^3 n_b \delta(\mathbf{p} - m_b \mathbf{v}), \quad (13)$$

where \mathbf{v} , m_b , and n_b denote the beam particle velocity, mass, and density, respectively [50]. The stopping power, i.e., $\partial\langle E\rangle/\partial x$ (where the x direction is considered to be parallel to the beam particle velocity \mathbf{v}), is then determined by the change of beam particle momentum per unit time.

Considering a homogeneous and isotropic target plasma [51] and low-density beams, i.e., neglecting intrabeam scattering and beam particle-beam particle correlations, we obtain for the stopping power of a partially ionized plasma

$$\begin{aligned} \frac{\partial}{\partial x}\langle E\rangle &= \frac{1}{n_b} \sum_c \int \frac{d\mathbf{p}}{(2\pi\hbar)^3} \frac{(\mathbf{p}\cdot\mathbf{v})}{v} I_{bc}(\mathbf{p}) \\ &+ \frac{1}{n_b} \sum_{cd} \int \frac{d\mathbf{p}}{(2\pi\hbar)^3} \frac{(\mathbf{p}\cdot\mathbf{v})}{v} I_{b(cd)}(\mathbf{p}). \end{aligned} \quad (14)$$

Here, the sums run over all elementary plasma species, i.e., electrons and the different ion species. Expression (14) considers all kinds of two- and three-particle processes that are included in the collision integrals I_{bc} and $I_{b(cd)}$, respectively. The bound state contributions are given by the second term. We consider only reactions in which the beam charge number remains constant, i.e., the beam particles enter and leave the scattering processes as free particles.

A. Ionization of plasma particles

The ionization of bound plasma particles by beam particle impact is described by two different terms of the three-

particle collision integral (4): The first one [$k=0$ in the second sum of Eq. (4)] is characterized by the set of distributions $f_b(\mathbf{p})F_j(\mathbf{P}_{ei})$ and the T matrix $T_{b(ei)}^{10}$. The second one is given by $k=1$ in the first sum of Eq. (4), i.e., by the set of distributions $f_1(k\bar{\alpha})=f_b(\bar{\mathbf{p}})F_j(\bar{\mathbf{P}}_{ei})$ and the T matrix $T_{b(ei)}^{01}$. Alternatively, the transition probability for the considered processes can be described by the three-particle T matrix $T_{b(ei)}^{11}$. However, the outgoing state includes a correlated scattering state of the ionized particle in this case [52],

$$\langle\mathbf{p}|\langle j\mathbf{P}_{ei}|T_{b(ei)}^{10}|\bar{\mathbf{p}}_i\rangle|\bar{\mathbf{p}}\rangle|\bar{\mathbf{p}}\rangle = \langle\mathbf{p}|\langle j\mathbf{P}_{ei}|T_{b(ei)}^{11}|\bar{\mathbf{P}}_{ei}\bar{\mathbf{p}}_e+\rangle|\bar{\mathbf{p}}\rangle. \quad (15)$$

Due to the large mass ratio of ions and electrons, i.e., $m_i/m_e \gg 1$, the argument of the ion distribution is then given by the center of mass momentum \mathbf{P}_{ei} , and the one for the electrons by the relative momentum \mathbf{p}_e .

The corresponding terms describing beam particle assisted recombination are proportional to three free particle distributions and can be neglected. With the beam particle distribution (13), we then obtain for the ionization contribution of the stopping power

$$\begin{aligned} \frac{\partial}{\partial x}\langle E\rangle^{\text{ion}} &= \frac{(2\pi\hbar)^6}{V\hbar} \sum_j \int \frac{d\mathbf{P}_{ei}}{(2\pi\hbar)^3} \frac{d\mathbf{p}}{(2\pi\hbar)^3} \frac{d\bar{\mathbf{P}}_{ei}}{(2\pi\hbar)^3} \frac{d\bar{\mathbf{p}}}{(2\pi\hbar)^3} \frac{d\mathbf{p}_e}{(2\pi\hbar)^3} \frac{(\mathbf{p}\cdot\mathbf{v})}{v} \\ &\times \{ \delta(E_{b(ei)}^0 - \bar{E}_{b(ei),j}^1) |\langle\mathbf{p}|\langle +\mathbf{p}_e\mathbf{P}_{ei}|T_{b(ei)}^{11}|\bar{\mathbf{P}}_{ei}j\rangle|\bar{\mathbf{p}}\rangle|^2 \delta(\bar{\mathbf{p}} - m_b\mathbf{v}) F_j(\bar{\mathbf{P}}_{ei}) \\ &- \delta(E_{b(ei),j}^1 - \bar{E}_{b(ei)}^0) |\langle\mathbf{p}|\langle j\mathbf{P}_{ei}|T_{b(ei)}^{11}|\bar{\mathbf{P}}_{ei}\mathbf{p}_e+\rangle|\bar{\mathbf{p}}\rangle|^2 \delta(\mathbf{p} - m_b\mathbf{v}) F_j(\mathbf{P}_{ei}) \}. \end{aligned} \quad (16)$$

We want to consider arbitrary mass ratios of plasma and beam ions. Therefore, it is appropriate to transform the momenta in Eq. (16) into Jacobi variables. These variables are defined by the following relations:

$$\mathbf{K} = \mathbf{p} + \mathbf{P}_{ei} \quad \text{and} \quad \mathbf{k} = \mathbf{p} - \frac{m_b}{M_{b(ei)}} \mathbf{K}, \quad (17)$$

where we have introduced the total mass of the three scattering particles $M_{b(ei)} = m_b + m_i + m_e$. The Jacobi coordinate \mathbf{K} is the center of mass momentum of the three-particle collision, and \mathbf{k} is the relative momentum between the beam particle and the bound state “(ei).” Due to the large mass ratio of ions and electrons, the third Jacobi momentum is given by the momentum of the ejected electron. We, therefore, keep the notation \mathbf{p}_e . In the further analysis, we will also use the total mass of the plasma particles $M_{ei} = m_i + m_e$ and the two reduced masses $\mu_b = m_b M_{ei} / M_{b(ei)}$ and $\mu_{ei} = m_e m_i / M_{ei}$.

For the three-particle T matrices $T_{b(ei)}^{11}$, we now obtain the relation

$$\begin{aligned} |\langle\mathbf{p}|\langle j\mathbf{P}|T_{b(ei)}^{11}|\bar{\mathbf{P}}\bar{\mathbf{p}}_e+\rangle|\bar{\mathbf{p}}\rangle|^2 &= (2\pi\hbar)^3 V \delta(\mathbf{K} \\ &- \bar{\mathbf{K}}) |\langle\mathbf{k}|\langle j|T_{b(ei)}^{11}|\bar{\mathbf{p}}_e+\rangle|\bar{\mathbf{k}}\rangle|^2 \end{aligned} \quad (18)$$

and for the three-particle energies, it holds

$$E_{b(ei)j}^1 = \frac{K^2}{2M_{b(ei)}} + \frac{k^2}{2\mu_b} + E_j + \Delta_b + \Delta_j, \quad (19)$$

$$E_{b(ei)}^0 = \frac{K^2}{2M_{b(ei)}} + \frac{k^2}{2\mu_b} + \frac{p_e^2}{2\mu_{ei}} + \Delta_b + \Delta_i + \Delta_e. \quad (20)$$

Again, E_j is the binding energy of the isolated two-particle bound state. Considering the arguments in the energy conserving δ function, it is useful to introduce the effective ionization energy of the bound state $|j\rangle$. This quantity is defined by

$$I_j^{\text{eff}} = |E_j| + \Delta_e + \Delta_i - \Delta_j. \quad (21)$$

Furthermore, it is convenient to define an auxiliary function g_b by

$$g_b^2 = k^2 - \frac{\mu_b}{\mu_{ei}} p_e^2 - 2\mu_b I_j^{\text{eff}}, \quad (22)$$

and to transform the momentum vectors \mathbf{k} and $\bar{\mathbf{k}}$ into polar coordinates. Therefore, we introduce the following angles $\angle(\mathbf{k}, \bar{\mathbf{k}}) = \theta$, $\angle(\mathbf{p}_b, \mathbf{k}) = \theta_1$, and $\angle(\mathbf{p}_b, \bar{\mathbf{k}}) = \theta_2$ and abbreviations $\cos \theta = x$, $\cos \theta_1 = x_1$, and $\cos \theta_2 = x_2$. These angles are not independent; they are connected by the well-known relation of spherical trigonometry $x_2 = xx_1 + \sin \theta \sin \theta_1 \cos \phi_x$.

Considering the conservation of total momentum and the expression (13) for the beam particle distribution, the \mathbf{K} and the $\bar{\mathbf{K}}$ integration can be performed easily. By utilizing also the energy conservation to perform the \bar{k} integration, we get for the stopping power the following intermediate result:

$$\begin{aligned} \frac{\partial}{\partial x} \langle E \rangle^{\text{ion}} &= \frac{1}{(2\pi)^4 \hbar^7} \frac{M_{ei}^3}{m_b^2} \int_0^\infty dk k^2 \int_{-1}^1 dx_1 x_1 \\ &\times F_j \left(M_{ei} \mathbf{v} - \frac{M_{b(ei)} \mathbf{k}}{m_b} \right) \\ &\times \int_0^\infty dp_e p_e^2 \int d\Omega_{p_e} \int_{-1}^1 dx g_b \\ &\times (k - g_b x) |\langle \mathbf{k} | \langle j | T_{b(ei)}^{11} | \mathbf{p}_e + \rangle | \bar{\mathbf{k}} \rangle|^2. \end{aligned} \quad (23)$$

Here, the modulus of the momentum $\bar{\mathbf{k}}$ is given by the function g_b , i.e., $|\bar{\mathbf{k}}| = g_b$. Following the usual definition of the total ionization cross section [53], we now define the momentum transfer or transport cross section of ionization by

$$\begin{aligned} Q_j^{\text{ion}}(k) &= \frac{\mu_b^2 g_b}{(2\pi)^2 \hbar^4 k} \int_0^\infty dp_e p_e^2 \int d\Omega_{p_e} \int_{-1}^1 dx \\ &\times \left(1 - x \frac{g_b}{k} \right) |\langle \mathbf{k} | \langle j | T_{b(ei)}^{11} | \bar{\mathbf{p}}_e + \rangle | \bar{\mathbf{k}} \rangle|^2. \end{aligned} \quad (24)$$

As we consider a nondegenerate target plasma in local thermal equilibrium, the distribution of bound plasma particles is given by the Boltzmann distribution. Therefore, the x_1 integration can be performed analytically, too. As the final result for the ionization contribution of the stopping power, we then obtain

$$\begin{aligned} \frac{\partial}{\partial x} \langle E \rangle^{\text{ion}} &= - \sum_j \frac{M_{ei}^2}{\mu_b^3} \frac{n_j \Lambda_{ei}^3}{(2\pi)^2 \hbar^3} \frac{k_B T}{v} \int_0^\infty dk k^3 Q_j^{\text{ion}}(k) \\ &\times \left\{ p_- \exp\left(-\frac{M_{ei} v_-^2}{2k_B T}\right) - p_+ \exp\left(-\frac{M_{ei} v_+^2}{2k_B T}\right) \right\}. \end{aligned} \quad (25)$$

Here, we have introduced the following abbreviations: $p_\pm = 1 \pm (\mu_b k_B T)/(M_{ei} k v)$ and $v_\pm = k/\mu_b \pm v$. Furthermore, $\Lambda_{ei} = (2\pi \hbar^2/M_{ei} k_B T)^{1/2}$ is the thermal wavelength of the composite plasma particles.

Expression (25) gives the stopping power due to the ionization of plasma particles in terms of the transport cross section of ionization. It has the same structure as the expression for the stopping power of fully ionized plasmas assuming statically screened interactions (see also Sec. IV). The different scattering processes are reflected by the different types of transport cross sections.

B. Excitation and deexcitation of plasma particles

Excitation and deexcitation processes as well as elastic collisions of beam particles with composite plasma particles are described by collision integrals that are characterized by a composite plasma particle in the input and output channels [$k=1$ term in the second sum of Eq. (4)]. The derivation of corresponding expressions for the stopping power is similar to the one shown in the previous section for the ionization contribution. However, we now have to introduce the transport cross section of (de)excitation:

$$\begin{aligned} Q_{jj'}^{\text{ex}}(k) &= \frac{\mu_b^2 g_b}{(2\pi)^2 \hbar^4 k} \int_{-1}^1 dx \left(1 - x \frac{g_b}{k} \right) \\ &\times |\langle \mathbf{k} | \langle j | T_{b(ei)}^{11} | j' \rangle | \bar{\mathbf{k}} \rangle|^2. \end{aligned} \quad (26)$$

The indices “ j ” and “ j' ” denote the internal quantum numbers of the incoming and the final state, respectively. Excitations of plasma particles are determined by the relation $E_j < E_{j'}$, whereas for deexcitations $E_j > E_{j'}$ holds. The transport cross section for elastic three-particle collisions has the same form but with $j = j'$.

Due to the different energy levels, we have to account for the fact that the excitation and deexcitation contributions have the opposite sign. Indeed, excitations of composite plasma particles reduce the beam energy while deexcitations deliver energy to the beam particles. Finally, we obtain for the contribution of the stopping power, which is due to excitation of composite plasma particles,

$$\begin{aligned} \frac{\partial}{\partial x} \langle E \rangle^{\text{ex}} &= - \sum_{E_i < E_{j'}} \frac{M_{ei}^2}{\mu_b^3} \frac{n_j \Lambda_{ei}^3}{(2\pi)^2 \hbar^3} \frac{k_B T}{v} \int_0^\infty dk k^3 Q_{jj'}^{\text{ex}}(k) \\ &\times \left\{ p_- \exp\left(-\frac{M_{ei} v_-^2}{2k_B T}\right) - p_+ \exp\left(-\frac{M_{ei} v_+^2}{2k_B T}\right) \right\}, \end{aligned} \quad (27)$$

where the same abbreviations are used as in Eq. (25). The deexcitation contribution has the opposite sign and the sum runs in this case over all states with $E_j > E_{j'}$. For the contribution due to the elastic scattering of the beam particle with a composite plasma particle and analogous expression can be obtained.

C. Limit of high beam particle velocities

In this section, we consider the contribution of three-particle collisions to the stopping power in the case of very energetic beam particles. First, we will focus on the ionization contribution. Our starting point is Eq. (23) but considerable simplification arise for fast beam particles. In this case, the relative momenta between the beam particle and the composite plasma particle before as well as after the collision, i.e., \mathbf{k} and $\bar{\mathbf{k}}$, are large compared to the momentum transfer defined by $\mathbf{q} = \mathbf{k} - \bar{\mathbf{k}}$. Therefore, the scattering angle θ is very small ($\cos \theta = x \approx 1$), too. Furthermore, we can assume that the energy of the ejected electron is small compared to the sum of kinetic beam and ionization energies. With the definition of the auxiliary function g_b (22), then, it follows that

$$k - g_b x \approx k - g_b, \quad (28)$$

$$\approx k - \sqrt{k^2 - 2\mu_b I_j^{\text{eff}}}, \quad (29)$$

$$\approx k^{-1} \mu_b I_j^{\text{eff}}. \quad (30)$$

Applying this approximation, we get for the stopping power

$$\begin{aligned} \frac{\partial}{\partial x} \langle E \rangle^{\text{ion}} &= \frac{1}{(2\pi)^2 \hbar^3} \sum_j I_j^{\text{eff}} \frac{M_{ei}^3}{\mu_b^2 m_b} \int_0^\infty dk k \\ &\times \sigma_j^{\text{ion}}(k) \int_{-1}^1 dx_1 x_1 F_j \left(M_{ei} \left[\mathbf{v} - \frac{\mathbf{k}}{\mu_b} \right] \right), \end{aligned} \quad (31)$$

where we have introduced the total ionization cross section. This quantity is defined by [53]

$$\begin{aligned} \sigma_j^{\text{ion}}(k) &= \frac{\mu_b^2 g_b}{(2\pi)^2 \hbar^4 k} \int_0^\infty dp_e p_e^2 \int d\Omega_{p_e} \\ &\times \int_{-1}^1 dx |\langle \mathbf{k} | \langle j | T_{b(ei)}^{11} | \bar{\mathbf{p}}_e + \rangle | \bar{\mathbf{k}} \rangle|^2. \end{aligned} \quad (32)$$

In this definition, the modulus of the momentum $\bar{\mathbf{k}}$ is fixed by the relation $\bar{k} = g_b$ and, therefore, a function of the ionization energy. Using the equilibrium (Boltzmann) distribution for the composite plasma particles, we obtain

$$\begin{aligned} \frac{\partial}{\partial x} \langle E \rangle^{\text{ion}} &= - \sum_j \frac{M_{ei}^2}{\mu_b^2} \frac{I_j^{\text{eff}} n_j \Lambda_{ei}^3}{(2\pi)^2 \hbar^3} \frac{k_B T}{v} \int_0^\infty dk k \sigma_j^{\text{ion}}(k) \\ &\times \left\{ p_- \exp\left(-\frac{M_{ei} v_-^2}{2k_B T}\right) - p_+ \exp\left(-\frac{M_{ei} v_+^2}{2k_B T}\right) \right\}. \end{aligned} \quad (33)$$

In the case of high beam velocities, the second term in the curly brackets is negligible. In the first term, only momenta with $k \approx \mu_b v$ contribute to the k integral. Furthermore, all functions can be treated as constant (at the point $k = \mu_b v$) compared to the strongly varying exponential. The remaining integral can be performed analytically. For the ionization contribution, the relation

$$\frac{\partial}{\partial x} \langle E \rangle^{\text{ion}} = - \sum_j I_j^{\text{eff}} n_j \sigma_j^{\text{ion}}(\mu_b v) \quad (34)$$

follows, where the sum runs over all existing bound states of composite plasma particles. From Eq. (34) we see the expected relations: the stopping power is proportional to the energy transfer per collision I_j^{eff} , the number density of the bound states in the plasma n_j , and the probability for an ionization. Nonideality effects are included by the medium dependent ionization energies I_j^{eff} and cross section σ_j^{ion} .

A similar expression can be found for processes that describe excitation of plasma particles. Compared to Eq. (34), the ionization energy has to be replaced by the excitation energy and the total excitation cross section σ_{jj}^{ex} has to be used in this case. Elastic collisions are negligible for high beam velocities. The same follows for the energy gain of the beam particles due to deexcitation of excited plasma particles because, for fast beam particles, the deexcitation process becomes unlikely compared to an ionization of the plasma particle.

To find an explicit expression for the high velocity limit of the stopping power, we need an analytic expression for the ionization cross section for large momenta or energies. For hydrogenlike composite particles, one can use a modified Bethe cross section (see, e.g., Refs. [23,54]). Comparing the cross sections for electron and ion impact, a scaling can be found. It turns out that, for the impact of energetic particles, the ionization cross section is only a function of the relative velocity. Furthermore, we found in the limit of large impact energies that the cross section is proportional to the square of the beam ion–electron interaction potential, i.e., $\sigma_j^{\text{ion}} \sim Z_b^2$. Therefore, we obtain for the ionization cross section at large impact energy

$$\sigma_j^{\text{ion}}(k) = 8 \pi a_B^2 Z_b^2 \frac{|E_j|}{m_e k^2 / 2\mu_b^2} \ln \left(\frac{2m_e k^2 / \mu_b^2}{|E_j|} \right), \quad (35)$$

where $|E_j|$ is the ionization energy of an isolated two-particle bound state. In contrast to the modified Bethe-Bibermann cross section suggested in Refs. [53,54], we neglect here the energy shifts in the logarithm because these terms are negligible for large impact energies.

Inserting the cross section (35) in Eq. (34), we obtain a generalized version of the Bethe formula for the ionization contribution of a hydrogenlike bound state. This expression is, in contrast to the original Bethe formula [23], also valid in the regime of strongly correlated plasmas,

$$\frac{\partial}{\partial x} \langle E \rangle^{\text{ion}} = -16\pi a_B^2 Z_b^2 \sum_j \frac{n_j I_j^{\text{eff}} |E_j|}{m_e v^2} \ln \left(\frac{2m_e v^2}{|E_j|} \right). \quad (36)$$

An analogous expression follows for the excitation contribution. The major nonideality effect on the stopping power in the high velocity limit is condensed in effective ionization energy I_j^{eff} . As this quantity is always smaller than the ideal ionization energy, the ionization contribution to the stopping power of a strongly coupled plasma is reduced compared to the one of a weakly coupled plasma with the same number density.

For target atoms or ions having more than one bound electron, we use the Bethe cross section [23]. For high impact energies, this cross section is proportional to the number of bound electrons. Therefore, we obtain for the stopping power of an ideal plasma

$$\frac{\partial}{\partial x} \langle E \rangle^{\text{ion}} = \frac{-4\pi Z_b^2 e^4}{m_e v^2} \sum_{Z=0}^{Z_c} (Z_c - Z) n_Z \ln \left(\frac{2m_e v^2}{|E_Z|} \right). \quad (37)$$

Here, Z_c denotes the nuclear charge of the considered target species, n_Z is the number density, and E_Z is the ionization energy of a (isolated) Z -fold charged ion. A similar formula was also found by Peter and Kärcher [27] for weakly coupled plasmas. It should be mentioned that Eq. (37) was successfully used to describe the energy loss of ions in weakly coupled, partially ionized plasmas with free electron densities $n_e < 10^{19} \text{ cm}^{-3}$ [8,9,28]. In a strongly coupled plasma, the reduction of the ionization energy, which is the major medium effect, can be included approximately by a factor $I_Z^{\text{eff}}/|E_Z|$ in every term of the sum.

D. Ionization and excitation cross section

We have shown in the previous sections that the ionization and excitation cross sections are the essential input quantities for the bound state contributions to the stopping power of partially ionized plasmas. In the case of very fast beam particles, the total ionization and excitation cross sections are needed for large impact energies and, therefore, a modified Bethe cross section could be utilized in Sec. III C. In the general case, we have to start from Eqs. (25) and (27). There, the transport cross sections of ionization and excitation are needed. These quantities are given in terms of the three-particle T -matrices $T_{b(ei)}^{11}$ according to the definitions (24) and (26).

As the solution of the effective three-body problem is a very difficult task, we apply here a Born approximation regarding the beam particle-plasma interaction, i.e., $T_{b(ei)}^{11} = V_{be} + V_{bi}$, but describing the output channel by a correlated scattering state $|\bar{\mathbf{p}}_e + \rangle$. Using this approximation, we obtain for the transport cross section of ionization

$$Q_j^{\text{ion}}(k) = \frac{\mu_b^2}{(2\pi)^2 \hbar^4 k^2} \int_0^{p_{\text{max}}} dp_e p_e^2 \int_{q_-}^{q_+} dq q \int d\Omega_{p_e} \times \left(1 - \frac{k^2 + q_b^2 - q^2}{2k^2} \right) |V_{be}(\mathbf{q}) P_{j,p_e}(\mathbf{q})|^2. \quad (38)$$

Here, the integration over the scattering angle has been transformed to an integration over the momentum exchange q . The limits of the q integration are given by the relation $q_{\pm} = k \pm \bar{k}$. The maximum momentum of the ejected electron follows from the energy conservation: $p_{\text{max}} = (m_e k^2 / \mu_b - 2m_e I_j^{\text{eff}})^{1/2}$. Furthermore, one has to consider that the modulus of $\bar{\mathbf{k}}$ is given by the auxiliary function g_b [see definition (22)].

In Eq. (38), dense plasma effects are taken into account by the statically screened beam particle-plasma electron interaction potential $V_{be}(\mathbf{q}) = 4\pi Z_b e^2 / (\kappa^2 + q^2 / \hbar^2)$, by an effective atomic form factor P_{j,p_e} , and the effective ionization energy I_j^{eff} . Considering the large mass difference of electrons and ions, the atomic form factor is given by

$$P_{j,p_e}(\mathbf{q}) = \int d\mathbf{r} \Psi_j^*(\mathbf{r}) \Psi_{p_e}(\mathbf{r}) \exp \left(-\frac{i}{\hbar} \mathbf{r} \cdot \mathbf{q} \right), \quad (39)$$

where $\Psi_j(r)$ and $\Psi_{p_e}(r)$ are the wave functions of the two-particle bound and scattering states determined by the Schrödinger equation with a statically screened interaction potential [33].

For the numerical evaluation, it is more convenient to use the angle integrated atomic form factors that are defined by

$$F_{(n,l),p_e}(q) = p_e^2 \int d\Omega_{p_e} |P_{j,p_e}(\mathbf{q})|^2. \quad (40)$$

The bound state is here characterized by the main quantum number n and the angular quantum number l . For a numerical evaluation of Eq. (40), we apply a partial wave expansion and get for the form factor

$$F_{(n,l),p_e}(q) = \frac{1}{k^2} \sum_{l',l''=0}^{\infty} \begin{pmatrix} l' & l'' & l \\ 0 & 0 & 0 \end{pmatrix} \begin{pmatrix} l' & l'' & l \\ 0 & 0 & 0 \end{pmatrix} \times (2l' + 1)(2l'' + 1) I_{(n,l),p_e}^{l',l''}(q), \quad (41)$$

where $\begin{pmatrix} l' & l'' & l \\ 0 & 0 & 0 \end{pmatrix}$ is a special Wigner 3- j symbol [55]. The quantity $I_{(n,l),p_e}^{l',l''}(q)$ is given by

$$I_{(n,l),p_e}^{l',l''}(q) = \left[\int_0^{\infty} dr u_{n,l}(r) u_{p_e,l'}(r) j_{l''}(qr/\hbar) \right]^2, \quad (42)$$

where $j_l(x)$ denotes the spherical Bessel function and $u_{n,l}(r)$ and $u_{p_e,l'}(r)$ are the radial wave functions for bound and scattering states, respectively. We computed these wave functions by numerical solution of the radial Schrödinger equation with a statically screened Coulomb potential and self-energy shifts in Debye approximation (see, e.g. [33,47,56]).

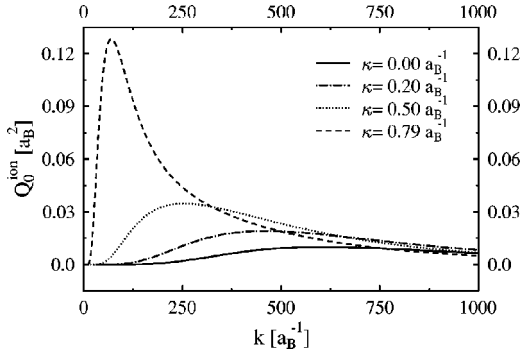


FIG. 1. Transport cross section of ionization $Q^{\text{ion}}(k)$ versus wave number $k=p/\hbar$ for different screening parameters κ . The considered process is the ionization of a hydrogen atom in the ground state by proton impact.

For the transport cross section of excitation, we obtain in the Born approximation

$$Q_{j,j'}^{\text{ex}}(k) = \frac{\mu_b^2}{(2\pi)^2 \hbar^4 k^2} \int_{q_-}^{q_+} dq q \times \left(1 - \frac{k^2 + q_b^2 - q^2}{2k^2} \right) |V_{be}(\mathbf{q}) P_{j,j'}(\mathbf{q})|^2. \quad (43)$$

Again, the limits of integration are given by $q_{\pm} = k \pm \bar{k}$, but the modulus of the momentum $\bar{\mathbf{k}}$ is now given by $\bar{k}^2 = k^2 - 2\mu_b I_j^{\text{eff}} + 2\mu_b I_{j'}^{\text{eff}}$. The corresponding atomic form factor for plasma particle excitation reads

$$P_{j,j'}(\mathbf{q}) = \delta_{j,j'} + \int d\mathbf{r} \Psi_j^*(\mathbf{r}) \Psi_{j'}(\mathbf{r}) \exp\left(-\frac{i}{\hbar} \mathbf{r} \cdot \mathbf{q}\right). \quad (44)$$

Numerical results for the transport cross section of ionization are plotted in Fig. 1 for different screening parameters. Here, the ionization of a hydrogen atom by proton impact is considered. The data for $\kappa=0$ are related to the Coulomb case or the weakly coupled high-temperature limit. Qualitatively, we find similar results as they were found for the total ionization cross section [33]: increasing screening lengths result in (i) a shift of the ionization threshold and of the maximum of the cross section to smaller wave vectors; (ii) an enhancement of the cross section in the region around the maximum; and (iii) a decrease of the cross section for large wave vectors k . The first and the second points are related to the lowering of the ionization energy with increasing screening length. Therefore, ionization requires less energy and is more likely. Compared to the screening effects in the case of electron impact [33], we observe here a much larger enhancement of the cross section. For large wave vectors, the weakening of the interaction potential by screening is the dominant effect, which gives rise to the opposite trend, i.e., a decreasing of the cross section.

IV. FREE PARTICLE CONTRIBUTION TO THE STOPPING POWER

To calculate the free particle contribution, we have to consider the first term on the rhs of Eq. (14). Elastic three-particle collisions are negligible. Depending on the beam velocity and the plasma parameters different effects are significant and, therefore, different approximation schemes for the two-particle collision integrals are appropriate.

In the important case of fast beam particles, dynamic screening effects and collective plasma excitation have to be included into the theory. These effects can be treated within the so-called V^S approximation [16]. Therefore, we have to apply the collision integral of the Lenard-Balescu equation [42,43] in Eq. (14). The resulting expression for the stopping power reads [17]

$$\frac{\partial}{\partial x} \langle E \rangle_{\text{RPA}}^{\text{free}} = \frac{2Z_b^2 e^2}{\pi v^2} \int_0^\infty \frac{dk}{k} \int_{(\hbar k^2/2m_b) - kv}^{(\hbar k^2/2m_b) + kv} d\omega \times \left[\omega - \frac{\hbar k^2}{2m_b} \right] \text{Im} \varepsilon^{-1}(k, \omega) n_B(\omega). \quad (45)$$

In this approximation, the stopping power is given in terms of the imaginary part of the inverse dielectric function ε^{-1} and the Bose function $n_B = [\exp(\hbar\omega/k_B T) - 1]^{-1}$ that represents the plasmon distribution. The dielectric function will be calculated here in random phase approximation (RPA). In the limit of very fast beam particles, the following formula can be obtained from Eq. (45):

$$\lim_{v \rightarrow \infty} \frac{\partial}{\partial x} \langle E \rangle^{\text{free}} = - \frac{Z_b^2 e^2 \omega_{pl}^2}{v^2} \ln \left(\frac{2m_e v^2}{\hbar \omega_{pl}} \right). \quad (46)$$

Here, $\omega_{pl}^2 = 4\pi e^2 \sum_c n_c / m_c$ denotes the square of the plasma frequency.

On the other hand, strong beam-plasma correlations are important for slow beam particles and strongly correlated plasmas. An appropriate approximation to describe these strong coupling effects is based on the T -matrix approximation for the collision integral of the quantum Boltzmann equation [44]. The corresponding expression for the stopping power is given in terms of the transport cross section for two-particle scattering Q_{bc}^T [17],

$$\frac{\partial}{\partial x} \langle E \rangle_{T\text{-matrix}}^{\text{free}} = - \sum_c \frac{m_c^2}{\mu_{bc}^3} \frac{n_e \Lambda_e^3}{(2\pi)^2 \hbar^3} \frac{k_B T}{v} \int_0^\infty dk k^3 Q_{bc}^T(k) \times \left\{ p_- \exp\left(-\frac{m_c v_-^2}{2k_B T}\right) - p_+ \exp\left(-\frac{m_c v_+^2}{2k_B T}\right) \right\}. \quad (47)$$

Here, $\mu_{bc} = m_b m_c / (m_b + m_c)$ is the reduced beam-plasma particle mass. The definitions for the abbreviations p_{\pm} and v_{\pm} are similar to the ionization case (see Sec. III A), but the reduced mass and the plasma particle mass have now to be replaced by μ_{bc} and m_c , respectively. The sum in Eq. (47) runs over all free carrier species in the plasma, but except for very slow beam particles only the free electrons have to be

considered. Dynamical screening effects are not included in the T -matrix calculation (47) because we apply a statically screened Coulomb potential to calculate the cross sections.

To incorporate both dynamic screening effects and strong beam-plasma correlations, a combined scheme for the stopping power was proposed in Ref. [16]. This model adds the RPA (45) and T -matrix (47) approximations and subtracts the static Born term to avoid double counting. In this way, the typical failures of the Born and static approximations for low and high beam velocities, respectively, can be avoided. The dynamic Born approximation (45), for instance, overestimates the stopping power several times for $v < v_{th}$ and strong beam-plasma coupling, i.e., low temperatures and large beam charge numbers [17,57]. On the other hand, the stopping power is underestimated by a factor of two applying the static approximation in the high velocity limit due to the neglect of plasmon excitation [16]. As the combined model is given by the T -matrix results (47) for $v \rightarrow 0$ and by the dynamic Born result (45) for very fast beam particles, it has the correct limiting behavior, which was shown by a comparison with simulation data and experiments [17,28]. For intermediate beam velocities, the combined model approximately accounts for both correlations and dynamical screening effects while smoothly interpolating between the static T matrix and the dynamically screened Born approximations. We therefore apply this combined scheme in this paper for the free particle contribution of the stopping power.

V. RESULTS AND DISCUSSION

A. Stopping power of partially ionized hydrogen plasma

1. Plasma composition

Beside the scattering cross sections, the plasma composition is the main input quantity to calculate the stopping power of partially ionized plasmas. Starting from the kinetic equations (3) and (11), rate equations for strongly coupled plasmas can be derived [33,34,53]. These equations determine the time evolution of the number densities of free and bound particles. In this paper, we consider target plasmas in thermodynamic equilibrium and, therefore, the rate equations reduce to a set of mass action laws. For a hydrogen plasma with atoms in the ground state follows

$$\frac{n_H}{n_e n_p} = \Lambda_e^3 \exp(\beta I_0^{\text{eff}}), \quad (48)$$

where $\beta = 1/k_B T$ is the inverse temperature. Following the definition (21), the effective ionization energy of the ground state is given by $I_0^{\text{eff}} = |E_0| + \Delta_e + \Delta_p - \Delta_0$ with $E_0 = -13.6$ eV being the ground state energy. The nonideality of the plasma is accounted for by the averaged energy shifts Δ_a (rigid shift approximation). Unfortunately, the simple Debye shift (7) is only justified for weakly coupled plasmas. In fact, this approximation overestimates the effect of screening, and pressure ionization is, therefore, predicted for too low densities.

Equation (48) describes the plasma composition determined by the ionization equilibrium of the reaction

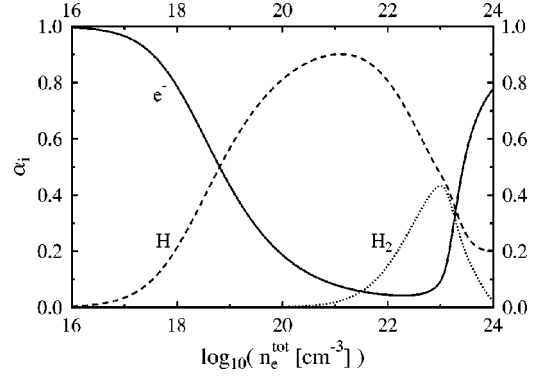


FIG. 2. Plasma composition of a hydrogen plasma with a temperature of $T = 2 \times 10^4$ K as a function of the total electron density. The quantity α_i is the fraction of the different species in units of the total electron density, i.e., $\alpha_e = n_e/n_e^{\text{tot}}$, $\alpha_H = n_H/n_e^{\text{tot}}$, and $\alpha_{H_2} = 2n_{H_2}/n_e^{\text{tot}}$.

$e + p \Leftrightarrow H$. Of course, this mass action law represents a rather simplified model to determine the plasma composition of hydrogen. In particular, at lower plasma temperatures, the formation of molecules, according to the dissociation equilibrium $H + H \Leftrightarrow H_2$, has to be taken into account.

To go beyond the approximations mentioned above, we apply the model introduced in Ref. [58]. In this scheme, the energy shifts are identified by the correlation part of the chemical potential, i.e., $\Delta_a = \mu_a^{\text{cor}}$. In the derived ionization-dissociation model, the plasma composition is determined by the following mass action laws:

$$n_H = 2n_p b_H^b \exp(\beta[\mu_e^{\text{id}} + \mu_e^{\text{cor}} + \mu_p^{\text{cor}} - \mu_H^{\text{cor}}]), \quad (49)$$

$$n_{H_2} = n_H^2 b_{HH}^b \exp(\beta[\mu_H^{\text{cor}} + \mu_H^{\text{cor}} - \mu_{H_2}^{\text{cor}}]). \quad (50)$$

Here, b_H^b denotes the partition sum of atomic bound states that is approximated by the ground state contribution, i.e., $b_H^b = \exp(-\beta E_0)$. b_{HH}^b is the bound state part of the fourth cluster coefficient for the electronic singlet state of atom-atom interaction. The contributions to the chemical potential that are due to interactions of free charged particles are calculated from Padé formulas. These formulas were determined on the basis of quantum statistical theory using the known limiting behavior for low and high densities as well as Monte Carlo data [48,59]. The charged particle-neutral scattering processes are included in terms of second cluster coefficients in first Born approximation using the optical potential method [60]. The contributions of neutral-neutral interactions are calculated in a simple manner from the Mansoori formula [61] applying temperature dependent hard sphere radii [58]. This scheme allows a qualitative description of neutral-neutral interaction in the considered temperature range of $T \geq 15\,000$ K. Of course, improvements are necessary, especially in the range of lower temperatures and high densities where atoms and molecules dominate the behavior of the system. This can be done using more realistic neutral-neutral interaction potentials (see, e.g., [62–64]).

Results for the plasma composition of a hydrogen plasma with a temperature of $T = 2 \times 10^4$ K are plotted in Fig. 2. For

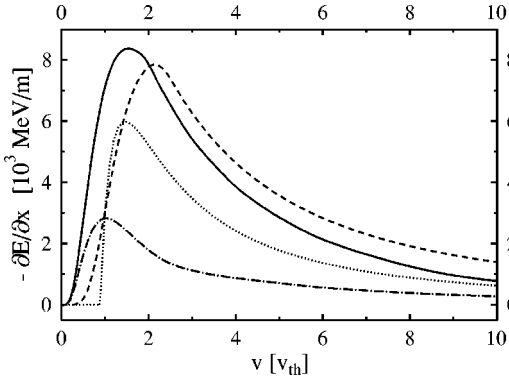


FIG. 3. Ionization contribution to the stopping power of a hydrogen plasma for a proton beam in different approximations (see text) versus beam particle velocity. The latter is given in units of the thermal velocity of the electron component $v_{\text{th}} = \sqrt{k_B T/m_e}$. The plasma temperature is $T = 10^5$ K and the total electron density is $n_e^{\text{tot}} = 5.5 \times 10^{22} \text{ cm}^{-3}$.

low densities, we get the behavior known for weakly coupled plasmas: an almost fully ionized plasma for very low densities and with increasing plasma density the formation of atoms (for $n_e^{\text{tot}} \geq 10^{17} \text{ cm}^{-3}$) and molecules (for $n_e^{\text{tot}} \geq 10^{21} \text{ cm}^{-3}$). Nonideality effects are small up to densities of $n_e^{\text{tot}} < 10^{21} \text{ cm}^{-3}$. For denser systems, the self-energy shifts reach the same magnitude as the dissociation and ionization energies. Therefore, the effective binding energies vanish and the bound states break up. We observe here the transition from a partially ionized to a fully ionized plasma due to pressure ionization. This behavior is known as the Mott transition [48]. As a result, most particles are free carriers for $n_e^{\text{tot}} > 5 \times 10^{23} \text{ cm}^{-3}$. Although this behavior is quite general, the density where the Mott transition occurs strongly varies for different approximations for the energy shifts Δ . Applying, e.g., the Debye shift (7), the Mott point occurs approximately one order of magnitude earlier.

2. Stopping power

Let us first discuss the ionization contribution to the stopping power separately. In Fig. 3, the ionization contribution of a hydrogen plasma is shown as a function of the beam velocity. The beam particles are protons and, therefore, the beam charge number is $Z_b = 1$. With the considered plasma temperature and density, an ionization degree of $\alpha = 0.74$ and a screening parameter of $\kappa = 0.49 a_B^{-1}$ follows. Hydrogen molecules are negligible in this case because their concentration is less than 1%. To test the influence of nonideality effects and to show the limitations of the often used Bethe formula, the following approximation schemes are plotted in Fig. 3: (i) the general expression (25) with the medium dependent transport cross section (38)—full line; (ii) the general expression (25) with the transport cross section (38) for the ideal case (that is $\kappa = 0$)—dashed line; (iii) the asymptotic formula (34) with the numerically calculated total ionization cross section in the Born approximation (32)—dash-dotted line; (iv) the asymptotic result (36) where the modified Bethe cross section (35) was utilized—dotted line.

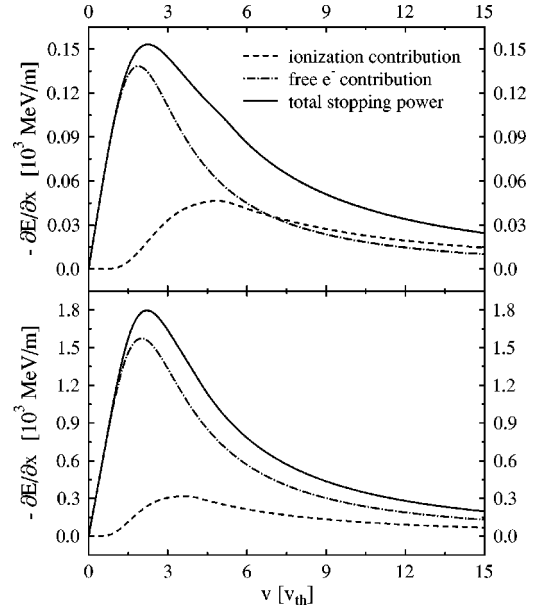


FIG. 4. Stopping power of a partially ionized hydrogen plasma for a proton beam versus beam particle velocity (in units of the thermal velocity of the electron component $v_{\text{th}} = \sqrt{k_B T/m_e}$). The plasma temperature and total electron density are $T = 2.0 \times 10^4$ K ($T = 3.5 \times 10^4$ K) and $n_e^{\text{tot}} = 10^{20} \text{ cm}^{-3}$ ($n_e^{\text{tot}} = 10^{21} \text{ cm}^{-3}$) in the upper (lower) figure, respectively.

It is clearly visible that both asymptotic results (iii) and (iv) underestimate the stopping power for low beam velocities. Although the energy threshold for ionization is calculated correctly within approximation (iii), the low-velocity region cannot be described. However, both asymptotic results merge for high beam particle velocities with the general result (i) that includes nonideality effects. A similar merger follows for fast beam particles if the nonideality corrections are neglected in all approximations (not shown). However, the results using ideal cross sections overestimate the energy loss in that case. This overestimation is a direct result of the neglect of screening effects, which ends up in too high cross sections in the large k -value domain (see Fig. 1).

Comparing the results (i) and (ii), one observes a shift to lower beam velocities if nonideality effects are considered. This shift follows from the lowering of the ionization energy. For this reason, beam particles with a lower energy (velocity) can ionize the target atoms in strongly coupled plasmas. This effect is not included in the ideal calculation (ii). The enhanced ionization probability in the low-energy domain (see Fig. 1) leads also to an enhancement in the stopping power for low beam velocities.

Figure 4 shows the total stopping power of a partially ionized hydrogen plasma, the free electron, and the ionization contributions as a function of the beam particle velocity. Again, the beam consists of protons, i.e., $Z_b = 1$. With the given plasma parameters, ionization degrees of $\alpha = 0.49$ and $\alpha = 0.19$ were obtained for the upper and lower figure, respectively. The molecule concentration is here again under 1%. Due to the fact that ionization requires a minimum impact energy, it is expected that the free electron contribution

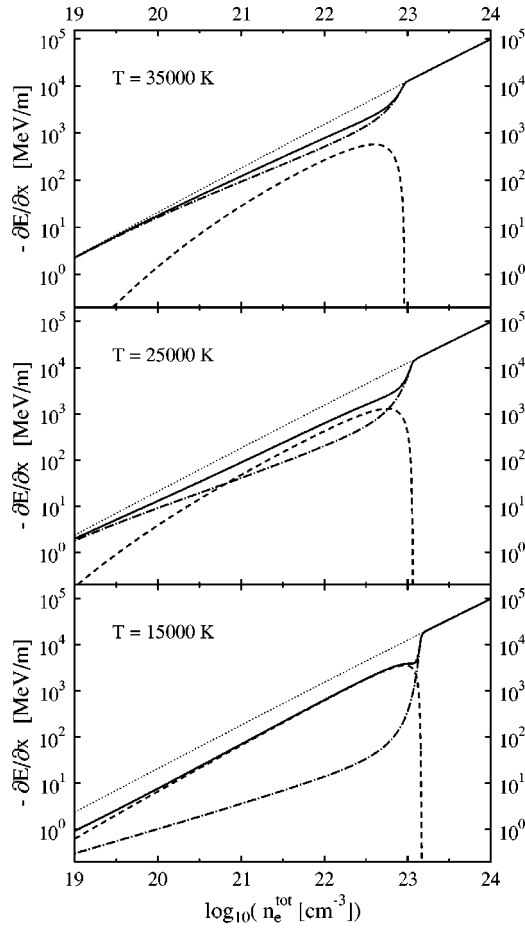


FIG. 5. Total stopping power (full line), free electron contribution (dash-dotted line), and ionization contribution (dashed line) of a partially ionized hydrogen plasma versus total electron density. The beam consists of protons with 1 MeV per particle. In addition, results assuming a fully ionized plasma (dotted line) are shown.

is dominant for very small beam velocities, which is confirmed by the numerical results in Fig. 4. However, our results show that also for beam energies where the maximum of the stopping power occurs, the free electrons give the major contribution even if only 19% of the electron are free carriers (see upper part). This behavior is even more pronounced in the case where the number of free electrons is approximately equal to the number of atoms. Here, the ionization of atoms contributes only 9% at the maximum of the total stopping power. This clearly shows that this effect, which is also known from weakly coupled plasmas, is much stronger in nonideal systems. The reason is that the energy transfer per collision, i.e., I_j^{eff} , is reduced by strong coupling effects.

For high beam velocities, the fraction of the ionization contribution becomes larger, but the contribution per bound electron is still smaller than the one per free electron. For instance, the contribution per free electron is approximately twice as high as the one per bound electron for a beam particle velocity of $v = 20 \times v_{\text{th}}$. As a result, the bound state contribution exceeds the free electron contribution for high velocities in the upper part of Fig. 4, but is noticeably

smaller in the lower part. Such an enhancement of the stopping power of plasmas compared to cold gases was also observed in experimental investigations of proton and deuteron stopping in plasmas [65,66] and can be explained with the different excitation energies in the corresponding high-velocity expressions, i.e., I_j^{eff} in Eq. (36) for the ionization contribution and $\hbar\omega_{\text{pl}}$ in Eq. (46) for the free plasma particles.

The density dependence of the stopping power is demonstrated in Fig. 5 for three different plasma temperatures. Hydrogen molecules are treated here as two (independent) atoms. The beam particles are protons with 1 MeV energy. Therefore, the high-velocity formula (36) can be used. To get a consistent description of plasma composition and stopping power, the effective ionization energy according to the model (49) and (50) is used in both calculations.

In addition to the total stopping power, the free electron and the ionization contributions are plotted. Furthermore, results for the stopping power assuming a fully ionized plasma are given for comparison. Due to the increasing number of both free and bound electrons with increasing total electron density, both contributions become larger in the low-density range. For very low densities, the plasma is approximately fully ionized. Therefore, the contribution of the bound electrons increases stronger due to the formation of atoms in the plasma with increasing density. As a result, a density region exists for $T = 1.5 \times 10^4$ K and $T = 2.5 \times 10^4$ K, where the stopping power due to ionization exceeds the free particle contribution. For $T = 3.5 \times 10^4$ K, the fraction of bound electrons is always too small to give a larger contribution than the free electrons.

A qualitatively different behavior can be observed at densities around $n_e^{\text{tot}} = 10^{23} \text{ cm}^{-3}$. Here, the ionization contribution suddenly drops. This behavior results from the simultaneous occurrence of two effects that both reduce this contribution. The first one is the lowering of the ionization energy that becomes significant in this region and reduces the energy transfer per collision. As the ionization energy also affects the plasma composition, second, the ionization degree increases rapidly. At the same density, the free electron contribution shows a strong increase because of the higher fraction of free electrons. As the free electrons give a higher contribution per particle than the bound electrons, the total stopping power shows a strong effective increase at this density, too. As we can see from the plasma composition (see Fig. 2), we observe here the transition from a partially ionized to a fully ionized plasma (Mott transition). The influence of this phenomenon on the stopping power of partially ionized plasmas is demonstrated here for a hydrogen plasma.

B. Stopping power of carbon and argon plasmas

For plasmas of elements other than hydrogen, one has to account for ions in different charge states. Consequently, it follows a set of coupled mass action laws for all possible charge states. In the nondegenerate case, we get instead of Eq. (48),

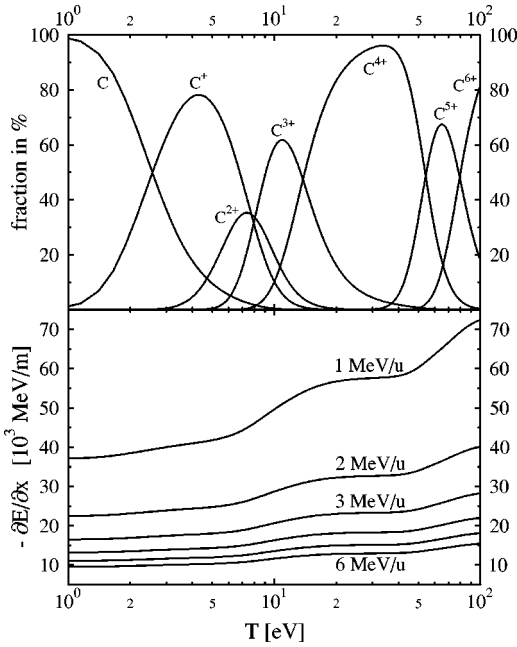


FIG. 6. Chemical composition (upper figure) and stopping power (lower figure) of a carbon plasma versus plasma temperature. The total nuclear density is $n_c^{\text{tot}} = 10^{21} \text{ cm}^{-3}$. In the lower figure, the stopping power is shown for different beam energies (velocities). The beam particle is a heavy ion with a charge state of $Z_b = 10$.

$$\frac{n_Z}{n_e n_{Z+1}} = \Lambda_e^3 \frac{g_Z}{g_{Z+1}} \exp(\beta I_Z^{\text{eff}}). \quad (51)$$

Here, n_Z is the number density of ions in the charge state Z and g_Z denotes the statistical weight. For the effective ionization energy I_Z^{eff} , we apply here a model proposed by Stewart and Pyatt [67] because of its numerical simplicity and proven good results for intermediate and high plasma temperatures [68]. This scheme smoothly interpolates between the Debye shifts for low densities and the ion-sphere model for high densities [67]. Again all atoms and ions are assumed to be in the ground state. The effective ionization energy of an ion in the charge state Z is given in this model by

$$I_Z^{\text{eff}} = |E_Z| - \frac{|3(\bar{Z} + 1)K + 1|^{2/3}}{2(\bar{Z} + 1)} k_B T. \quad (52)$$

Here, \bar{Z} is the average charge state of the ions, and the parameter K is defined as $K = \bar{Z} e^2 \kappa / k_B T$.

In the upper part of Fig. 6, results for the chemical composition of a carbon plasma are presented as a function of the plasma temperature. Qualitatively, we find the expected results: almost only atoms exist at low temperatures; then the ionization degree increases with the temperature. All ionization stages appear and disappear at certain temperatures and only sixfold ionized carbon ions exist for very high temperatures. However, the fractions of the different ions species are influenced by correlation effects, especially in the temperature range where the maximum of the C^+ and the C^{2+} ions occurs. Here, the composition is noticeably modified com-

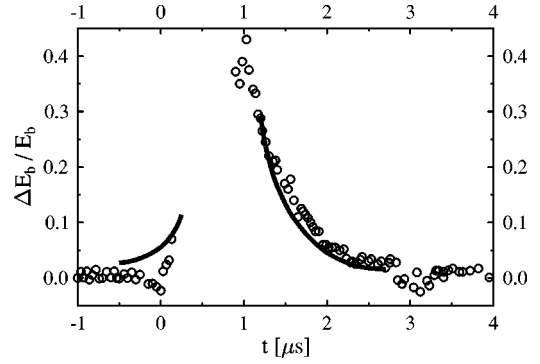


FIG. 7. Energy loss of a $^{238}\text{U}^{53+}$ ions with a beam energy of 6.3 MeV per nucleon traveling through a 20 cm long, partially ionized argon plasma. The theoretical result is plotted as a full line. The circles show experimental results taken from Ref. [69].

pared to an ideal calculation. Furthermore, we want to point out that the very stable configuration of the (heliumlike) C^{4+} ions dominates in a large temperature range. These plasma temperatures are of special interest to describe beam-plasma interaction experiments where C^{4+} ions were also detected spectroscopically [29].

The influence of the chemical composition on the stopping power of a carbon plasma is demonstrated in the lower part of Fig. 6 for fast beam ions (1, 2, 3, 4, 5, and 6 MeV per nucleon beam energy). Obviously, the stopping power increases with the plasma temperature (or the ionization degree). This increase is again explained by the fact that the free electrons give a higher contribution per electron than the bound ones. As this different behavior is more pronounced at lower beam velocities, we observe a stronger increase in this case. A remarkable increase occurs for temperatures around $T = 10 \text{ eV}$ where the ionization degree changes more rapidly. This range is then followed by plateaulike region from $T \approx 15 \text{ eV}$ to $T \approx 40 \text{ eV}$, which is a direct effect of the stable heliumlike configuration resulting in an almost constant ionization degree.

A comparison of our theoretical predictions with experimental results is given in Fig. 7, where data for the energy loss of ^{238}U ions traveling through a 20 cm long, partially ionized argon plasma are shown [8,69]. The plasma was produced using a Z pinch with a pinch-axis parallel to the beam direction. The lack in the experimental data is due to the strong reduction of the output beam intensity, which is an effect of the strong focusing force of the plasma current (plasma lens effect) [70]. It was shown experimentally that the beam ion charge number remains almost constant around $Z_b = 53$. The beam particle energy is 6.3 MeV per nucleon that justifies the application of the high-energy formulas (37) and (46). However, it should be mentioned that strong fields can influence the stopping power due to the free electrons (see, e.g., Refs. [71,72] for magnetic fields).

The densities of the free electrons were taken from time-resolved spectroscopy measurements and are in the range of $n_e = 10^{18} - 10^{19} \text{ cm}^{-3}$. Assuming a plasma temperature of $T = 10^5 \text{ K}$, the (time dependent) total nuclear densities are then calculated from the solution of the set of Saha equations (51). This calculation does not include the effects of electro-

magnetic fields and also neglects the heating and cooling of the plasma during the pinch and the relaxation phases, respectively. It should be mentioned that a considerable increase of the ionization degree due to electric fields occurs, in the given electron density range, only for field strengths $E > 10^6$ V/m [73] whereas magnetic fields tend to decrease the ionization degree [74]. It can also be shown that the total stopping power is only a weak function of the plasma temperature for $T \geq 10^5$ K [8]. Since the average charge state of the plasma ions never exceeds $\bar{Z} = 5$, the main contribution to the energy loss is due to the ionization of bound electrons.

The comparison shows a good agreement between the calculated and the measured stopping power in the expansion phase that verifies the applicability of the high velocity result (37) for plasmas with densities up to $n_c = 10^{19}$ cm⁻³. The disagreement in the compression phase is mainly due to the fact that the temperature is not constant during the discharge but strongly increases during the compression.

VI. SUMMARY

We developed a kinetic approach for the stopping power of partially ionized plasmas that is based on quantum kinetic equation. The derived expressions are valid for arbitrary beam particle velocities. Furthermore, a generalized Bethe formula for fast beam particles was derived. With this kinetic approach, we were able to include all relevant types of two-

and three-particle collisions as well as the influence of correlation effects. Special attention was paid to the bound state contribution of the stopping power where ionization and excitation of a composite plasma particles by beam particle impact were considered. In particular, the nonideality effects on the cross sections were discussed. Then these results were used to calculate the stopping power of partially ionized hydrogen plasmas. The largest nonideality effects were found for low beam velocities. Especially, the threshold for the ionization was shifted to smaller beam velocities. For fast beam particles, we found a reduction of the stopping power due to the lowering of the ionization energy. Furthermore, we observed the Mott transition in the stopping power for large densities. The effect of temperature ionization on the stopping power was demonstrated for a carbon plasma. Finally, we have shown a comparison with experimental data for an argon plasma that proves the applicability of the Bethe-like formula for fast ion beams.

ACKNOWLEDGMENTS

This work was supported by the Deutsche Forschungsgemeinschaft (Sonderforschungsbereich 198 “Kinetik partiell ionisierter Plasmen”) and the U.S. Department of Energy. D.G. gratefully acknowledges support from the German Academic Exchange Service (DAAD).

-
- [1] *Energy From Inertial Fusion*, edited by W. J. Hogan (International Atomic Energy Agency, Vienna, 1995).
 - [2] Proceedings of the 12th International Symposium on Heavy Ion Inertial Fusion, Heidelberg, 1997, edited by I. Hofmann and H. J. Bluhm [Nucl. Instrum. Methods, Phys. Res. A **415** (1998)].
 - [3] A. M. Oparin, S. I. Anisimov, and J. Meyer-ter-Vehn, Nucl. Fusion **36**, 443 (1996).
 - [4] D. G. Hicks *et al.*, Phys. Plasmas **7**, 5106 (2001).
 - [5] M. Roth *et al.*, Phys. Rev. Lett. **86**, 436 (2001).
 - [6] U. Neuner *et al.*, Phys. Rev. Lett. **85**, 4518 (2000).
 - [7] N. A. Tahir *et al.*, Phys. Rev. E **63**, 016402 (2001).
 - [8] H. Wetzler, W. Süss, C. Stöckl, A. Tauschwitz, and D. H. H. Holfmann, Laser Part. Beams **15**, 449 (1997).
 - [9] A. Golubev *et al.*, Phys. Rev. E **57**, 3363 (1998).
 - [10] X.-Z. Yan, S. Tanaka, S. Mitake, and S. Ichimaru, Phys. Rev. A **32**, 1785 (1985).
 - [11] I. Nagy, A. Arnau, and P. M. Echenique, Phys. Rev. A **40**, 987 (1989).
 - [12] E. Zaremba, A. Arnau, and P. M. Echenique, Nucl. Instrum. Methods Phys. Res. B **96**, 619 (1995).
 - [13] J. W. Dufty and M. Berkovsky, Nucl. Instrum. Methods Phys. Res. B **96**, 626 (1995).
 - [14] O. Boine-Frankenheim, Phys. Plasmas **3**, 792 (1996).
 - [15] W. D. Kraeft and B. Strege, Physica A **149**, 313 (1988).
 - [16] D. O. Gericke, M. Schlanges, and W. D. Kraeft, Phys. Lett. A **222**, 241 (1996).
 - [17] D. O. Gericke and M. Schlanges, Phys. Rev. E **60**, 904 (1999).
 - [18] G. Zwicknagel, P.-G. Reinhard, C. Seele, and C. Toepffer, Fusion Eng. Des. **32-33**, 395 (1996).
 - [19] G. Zwicknagel, C. Toepffer, and P.-G. Reinhard, Phys. Rep. **309**, 117 (1999).
 - [20] N. R. Arista, Phys. Rev. B **18**, 1 (1978).
 - [21] C. Deutsch and P. Fromy, Phys. Rev. E **51**, 632 (1995).
 - [22] N. Bohr, Philos. Mag. **25**, 1913 (1916).
 - [23] H. Bethe, Ann. Phys. (Leipzig) **5**, 325 (1930).
 - [24] F. Bloch, Ann. Phys. (Leipzig) **16**, 285 (1933).
 - [25] M. M. Basko, Fiz. Plazmy **10**, 1195 (1984) [Sov. J. Plasma Phys. **10**, 689 (1984)].
 - [26] Th. Peter and J. Meyer-ter-Vehn, Phys. Rev. A **43**, 2015 (1991).
 - [27] Th. Peter and B. Kärcher, J. Appl. Phys. **69**, 3835 (1991).
 - [28] C. Stöckl *et al.*, Laser Part. Beams **14**, 561 (1996).
 - [29] M. Roth, C. Stöckl, W. Süss, O. Iwase, D. O. Gericke, R. Bock, D. H. H. Hoffmann, and W. Seelig, Europhys. Lett. **50**, 28 (2000).
 - [30] M. Schlanges, D. O. Gericke, W. D. Kraeft, and Th. Bornath, Nucl. Instrum. Methods Phys. Res. A **415**, 517 (1998).
 - [31] D. Kremp, M. Schlanges, and Th. Bornath, in *The Dynamics of Systems with Chemical Reactions*, edited by J. Popielawski (World Scientific, Singapore, 1989).
 - [32] Th. Bornath, D. Kremp, W. D. Kraeft, and M. Schlanges, Phys. Rev. E **54**, 3274 (1996).
 - [33] M. Schlanges and Th. Bornath, Physica A **192**, 262 (1993); Th. Bornath and M. Schlanges, *ibid.* **196**, 427 (1993).
 - [34] Th. Bornath, M. Schlanges, and R. Prenzel, Phys. Plasmas **5**, 1485 (1998).

- [35] S. W. Peletminskii, Zh. Teor. Mat. Fiz. **6**, 123 (1971) [Theor. Math. Phys. **6**, 88 (1971)].
- [36] Yu. L. Klimontovich and D. Kremp, Physica A **109**, 517 (1981).
- [37] Yu. L. Klimontovich, D. Kremp, and W. D. Kraeft, Adv. Chem. Phys. **58**, 175 (1987).
- [38] Yu. L. Klimontovich, M. Schlanges, and Th. Bornath, Contrib. Plasma Phys. **30**, 349 (1990).
- [39] D. Kremp, M. Schlanges, and Th. Bornath, Phys. Status Solidi B **147**, 747 (1988).
- [40] M. Schlanges and Th. Bornath, Contrib. Plasma Phys. **37**, 239 (1997).
- [41] Th. Bornath, M. Schlanges, F. Morales, and R. Prenzel, J. Quant. Spectrosc. Radiat. Transf. **58**, 501 (1997).
- [42] A. Lenard, Ann. Phys. (N.Y.) **3**, 390 (1960).
- [43] R. Balescu, Phys. Fluids **3**, 52 (1960).
- [44] P. Danielewicz, Ann. Phys. (N.Y.) **152**, 239 (1984).
- [45] J. R. Taylor, *Scattering Theory* (Wiley, New York, 1972).
- [46] C. J. Joachain, *Quantum Collision Theory* (North-Holland, Amsterdam, 1975).
- [47] R. Zimmermann, *Many-Particle Theory of Highly Excited Semiconductors* (Teubner, Leipzig, 1987).
- [48] W. D. Kraeft, D. Kremp, W. Ebeling, and G. Röpke, *Quantum Statistics of Charged Particle Systems* (Plenum, New York, 1986).
- [49] H. D. Betz, Rev. Mod. Phys. **44**, 465 (1972).
- [50] From this point, we use the index “*b*” to indicate beam particle properties.
- [51] Weak spatial deviations of the plasma parameters can be incorporated considering local particle densities and temperatures, but the effects of weak electric or magnetic fields are not included.
- [52] Th. Bornath, M. Schlanges, and D. Kremp, Contrib. Plasma Phys. **28**, 57 (1988).
- [53] M. Schlanges, Th. Bornath, and D. Kremp, Phys. Rev. A **38**, 2174 (1988).
- [54] L. M. Biberman, V. S. Vorobev, and I. T. Iakubov, *Kinetics of the Nonequilibrium Low-Temperature Plasma* (Consultants Bureau, New York, 1987).
- [55] L. D. Landau and E. M. Lifschitz, *Course of Theoretical Physics* (Pergamon Press, Oxford, 1976), Vol. III.
- [56] D. O. Gericke, M. Schlanges, and W. D. Kraeft, Laser Part. Beams **15**, 523 (1997).
- [57] D. O. Gericke, M. Schlanges, Th. Bornath, and W. D. Kraeft, Contrib. Plasma Phys. **41**, 147 (2001).
- [58] M. Schlanges, M. Bonitz, and A. Tschtschjan, Contrib. Plasma Phys. **35**, 109 (1995).
- [59] W. Ebeling and W. Riechert, Ann. Phys. (Leipzig) **39**, 362 (1982).
- [60] P. Haronska, D. Kremp, and M. Schlanges, Wiss. Z. Univ. Rostock **36**, 98 (1987).
- [61] G. A. Mansoori, N. F. Carnahan, K. E. Starling, and T. W. Leland, J. Chem. Phys. **54**, 1523 (1971).
- [62] M. Ross, F. H. Ree, and D. A. Young, J. Chem. Phys. **79**, 1487 (1983).
- [63] F. H. Ree, in *Shock Waves in Condensed Matter*, edited by S. C. Schmidt and N. C. Holmes (Elsevier, New York, 1988).
- [64] F. J. Rogers, Contrib. Plasma Phys. **41**, 179 (2001).
- [65] F. C. Young, D. Mosher, S. J. Stephanakis, S. A. Goldstein, and T. A. Mehlhorn, Phys. Rev. Lett. **49**, 549 (1982).
- [66] J. N. Olsen, T. A. Mehlhorn, J. Maenchen, and D. J. Johnson, J. Appl. Phys. **58**, 2958 (1985).
- [67] J. C. Stewart, and K. D. Pyatt, Astrophys. J. **144**, 1203 (1966).
- [68] R. Fehr, M. Schlanges, and W. D. Kraeft, Contrib. Plasma Phys. **39**, 81 (1999).
- [69] H. Wetzler, C. Stöckl, W. Seehg, J. Jacoby, and D. H. H. Hoffmann, in *Physics of Strongly Coupled Plasmas*, edited by W. D. Kraeft and M. Schlanges (World Scientific, Singapore, 1996), p. 357.
- [70] D. H. H. Hoffmann *et al.*, Radiat. Eff. Defects Solids **126**, 345 (1993).
- [71] H. B. Nersisyan, Phys. Rev. E **58**, 3686 (1998).
- [72] M. Steinberg and J. Ortner, Phys. Rev. E **63**, 046401 (2001).
- [73] D. Kremp, K. Morawetz, M. Schlanges, and V. Rietz, Phys. Rev. E **47**, 635 (1993).
- [74] M. Steinberg, J. Ortner, and W. Ebeling, Phys. Rev. E **58**, 3806 (1998).